Archives available at journals.mriindia.com

International Journal on Advanced Computer Engineering and Communication Technology

ISSN: 2278-5140

Volume 15 Issue 01, 2026

Optimized Deep Transfer Learning Based Detection and Diagnosis of Parkinson's Disease

T. Krishnaswamy
Department of Electronics and Communication Engineering, Arunachala College of Engineering for Women, Vellichanthai, Tamilnadu, India

Peer Review Information

Submission: 20 April 2026
Revision: 15 May 2026
Acceptance: 27 May 2026

Keywords

Parkinson's Disease, Early Disease Detection, Deep Learning, Handwritten Document Analysis, Genetic Algorithm, Feature Optimization, K-Nearest Neighbour (KNN), Chronic Disease Diagnosis, Machine Learning, Precision and Accuracy.

Abstract

The symptoms of Parkinson's disease (PD), a chronic neurological condition, are similar to those of other illnesses and advance slowly. It is essential to diagnose Parkinson's disease (PD) early in order to provide the right medication for patients to lead healthy, productive lives. In addition to various mental symptoms, the disease is characterised by tremors, muscle rigidity, slowness in movements, and abnormalities in balance. One of the primary factors that facilitate PD detection and evaluation is the dynamics of handwritten documents. For the early detection of this illness, a number of machine learning techniques have been studied. The majority of these manually developed feature extraction methods, however, primarily struggle with poor performance accuracy. When dealing with the discovery of a chronic illness like this, this cannot be tolerated. An effective deep learning model is therefore put out, which can help with Parkinson's disease early diagnosis. The suggested model's key contribution is its ability to choose the best features, which results in high performance accuracy. The K-Nearest Neighbour approach is used in a genetic algorithm to optimise the features. The suggested innovative model yields an area under the curve of 0.90 with a loss of 0.12 only, a detection accuracy of over 95%, and a precision of 98%. The superior detection capabilities of our model is demonstrated by comparing its performance with some cutting-edge machine learning and deep learning-based PD detection techniques.

Introduction

In 500 km electrical power systems, a wide range of reactive power adjustment is achieved to mitigate voltage imbalance. The unbalance load fluctuations must be minimised to a reasonable level (often less than 2%) using an Optimal Control Technique (OCT) that covers a wide range of Voltage Unbalance Factor (VUF), from 3.33% to 12.4601% [1]. This study suggests a three-layer hierarchical control methodology as the best multiobjective method for controlling the active and reactive power supplied by distributed generators in low-voltage microgrids. Prior knowledge of network parameters is not required for this method [2]. Under healthy operating conditions, the series inverter and shunt inverter both contribute to load reactive power compensation because of the phase angle shift. By minimising three objective functions, the suggested method finds the ideal site, the ideal reactive power compensation needed there, and the ideal UPQC design parameters [3]. In addition to providing essential frameworks for energy production and distribution to end users, ancillary services include reactive power services, which are essential for regulating bus voltage. Among the many ancillary services needed in a market with competition, the provision of enough reactive electricity to ensure grid safety and voltage stability is crucial [4]. Exploring how dynamic loads, such as induction motors, behave at steady

state operation as the reactive power requirement of the supply increases is the aim of this study. It also examines how the network that provides these loads is impacted by this demand fluctuation [5]. This study presents a comprehensive review of the literature on reactive power management in power networks with substantial renewable resources. In order to assess REGs' compatibility for future network demands, an overview of the reactive power requirements for REGs described in different grid codes is given [6]. Analysing the data produced by different writers for different objective functions identifies a scientific problem in the dispute that the electric variables exhibit when examined separately. This shows that the problem needs to be analysed using multiple criteria and that distribution grid topologies with distributed generation and energy storage should be taken into consideration [7]. For this method to be effective, prior knowledge of network parameters is not required. The multiobjective algorithm is employed at the secondary level to maximise active power generation and minimise reactive power circulation & current imbalance in order to achieve optimal dispatch [8]. In order to calculate the operating conditions of the EPS, the suggested methodology applies the ideal AC power flows as a basis to each power phase [9]. The implementation of a distributed control architecture that prioritises DRES response to keep network voltages within acceptable bounds and reduce network losses is another unique aspect of this system [10]. Due to the increased demand for power, there are issues with voltage drops, especially when it comes to the quality of the voltage at times of peak load [11]. This paper reviews the research on reactive power management in power networks using renewable resources. In order to assess their ability to meet future network demands, the reactive power needs of REGs as defined by different grid codes are gathered [12]. This article's noteworthy contributions include the following:

- During the pre-processing phase, we first improved the difference of a specific input image using the image contrast enhancement technique. The supplied image's noise was then removed using the mean filter. Subsequently, we employed the multi-scale morphological gradient approach to mix and filter the contrast-enhanced image into a single fused image.
- We presented a brand-new Pyramid channel-based feature attention network (PCFAN) that extracted the preprocessed image's features using a multi-stage design with attention blocks at each step.
- To improve the accuracy of PD level categorisation, including mild, moderate, and severe, we combined the Dwarf Mongoose Optimisation approach with the MobileNetV3 technology.
- The PPMI and NTUA databases have been the subject of numerous ablation experiments. The experimental findings demonstrated that, in comparison to all other approaches, the proposed network performed better than the state efficiency.

Related Works

Along with a review of recent studies on the machine learning algorithms used in PD categorisation, this section discusses the most recent deep learning techniques. A 1D convolutional neural network (1D-Convnet) was created by El Maachi, Bilodeau, and Bouachir (2020) to analyse gait data and provide a DNN classifier for Parkinson's disease. It processes 18 parallel 1D data points from foot sensors that detect the vertical ground response force (VGRF). System inputs are represented by 18 parallel 1D-Convnets in the first segment of the network. The final classification is generated in the second component, a fully linked network, by concatenating the output of the 1D-Convnets. According to our tests, the recommended method effectively identifies Parkinson's disease using gait data. The suggested method's accuracy percentage was 98.7%. Loh et al. (2021) used deep learning to create a 2D-CNN model that can automatically diagnose Parkinson's illness. Using the suggested 2D-CNN model, the technique employed in this work to identify Parkinson's disease successfully separated spectral images into healthy controls and unaffected PD patients with or without dopamine-producing medications. The suggested model obtained a high accuracy of 99.46% when multi-categorization was performed using tenfold cross-validation. A method for PD identification using CNN and isosurface-based characteristics was proposed by Ortiz et al. (2019). Based on LeNet-5 and AlexNet, they employed a convolutional neural network (CNN) model to identify isosurfaces and extract descriptive information. Isosurfaces connect voxels with a certain intensity or value, much like contour lines connect locations of identical height. The endeavour resulted in the development of a categorisation system that classified DaTSCAN images using supervised learning through CNN architectures. Deep CNNs were developed by

Karaman et al. (2021) to automatically detect Parkinson's disease (PD) from voice sounds derived from biomarkers. The well-known CNN algorithms had two primary stages: fine-tuning-based transfer learning techniques and data pre-processing.They investigated if combining a voice dataset from a large dataset with transfer learning model fine-tuning techniques may improve PD identification. According to the findings, the suggested deep CNN model, which combines transfer learning with a fine-tuning technique, has a 91.17% accuracy rate in identifying Parkinson's disease.

A unique classification framework was developed by Diaz et al. (2021) employing one-dimensional convolutions and bidirectional gated recurrent units (BiGRU) to investigate the potential for handwriting's sequential information for Parkinson's symptom diagnosis. Once the generated sequences had passed one-dimensional convolutions on the raw sequences and derived features, they were fed to BiGRU layers to create the final classification in this study. Comparatively speaking, the suggested strategy fared better than the other available options. Olivares et al. (2020) developed an improved ELM by utilising the Bat Algorithm, which extends the computer learning technique's training phase to increase accuracy while lowering or maintaining loss in the learning phase. An optimal vector is simultaneously defined using the approximation technique with input weights and bias values. In order to generate the optimum categorisation model, it aims to optimise the ELM's training phase. In comparison to current methods, the suggested methodology produces better results. Using deep learning (DL) techniques, Vyas et al. (2022) provided two novel approaches. We used 2D and 3D convolution neural networks (CNNs) trained on axial-plane MRI data. The algorithm was made more effective by performing four pre-processing steps: picture scaling, z-score normalisation, histogram matching, and N4 bias correction. The test data was successfully classified by the 3D model with an accuracy of 88.9% & an area under the curve (AUC) of 0.86.

Proposed Methodology

Three stages make up the suggested methodology: preprocessing, feature extraction, and classification. The initial step in the pre-processing procedure was to boost the contrast of the input image using the image contrast enhancement method. The noise was then eliminated using a mean filter. The filtered and contrast-enhanced photos were combined into a single image using a multi-scale morphological gradient approach to create the fused image. We introduced a new Pyramid channel-based feature attention network (PCFAN) that used a multi-stage design with attention blocks at each level to extract the features from the preprocessed picture.Finally, using MobileNetV3, the photos were categorised as mild, moderate, and severe. The IDMO algorithm optimised the hyperparameters of the classification strategy. The suggested methodology's architecture diagram is shown in Figure 1.

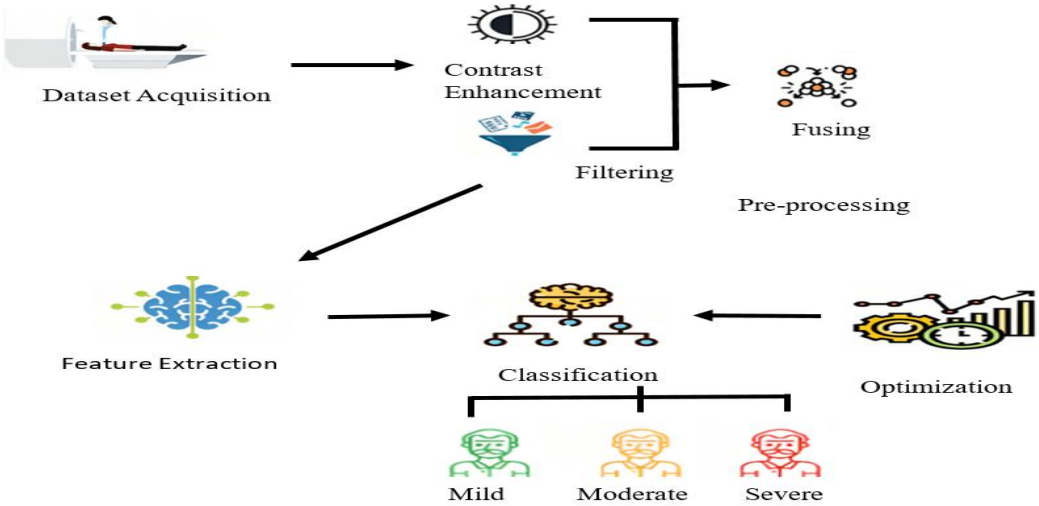

Figure 1: Proposed Architecture Diagram

The best exposure ratio was then found for locations where the original image was underexposed such that the synthetic image was adequately exposed. In order to produce a better image, the input and generated images were further combined using a weight matrix. This approach relied on the fundamental formulas found in equations (1) and (2). The photos were

combined using Eq. (4) to produce a pixel-by-pixel image.

$$R^c = \sum_{i=1}^{N} W_i P_i^c \quad (1)$$

N denotes image quality, whereas PiPi is the exposure set's i-th image. R stands for the result of the enhancement, c for the three-color channel index, and WiWi for the image's weight map. To calculate PiPi, use Equation (2).

$$P_i = g(P, k_i) \quad (2)$$

K_i is the exposure ratio, while g is the brightness transform function (BTF). The beta-gamma connectivity method, which was developed from Equation (3), served as the BTF in our investigation.

$$g(P, K) = \beta P^{\gamma} = e^{b(1-k^a)} P^{(k^a)} \quad (3)$$

The variables a, b, and k of the camera could be used to compute the parameters β and γ. As in the original study, we employed a constant parameter (a = 0.3293; b = 1.158). At the conclusion of the process, the enhanced image was produced using Equation (4).

$$R^c = WP^c + (1 - W)g(P^c, k) \quad (4)$$

1. Mean filtering

Picture de-noising in the spatial domain usually involves graphic convolution processing with multiple picture flattening patterns. Replace the single grey value of a pixel with the sum of the grey values of all nearby pixels to form the basis of mean filtering. The procedure as follows: An image is made for a pixel point (a, b) in a source picture with f (a, b), and there are M pixels in the area S around it:

$$G(x, y) = \frac{1}{M} \sum_{(i,j \in S)} f(a, b)(a, b) \notin S \quad (5)$$

2. Multi-scale morphological gradient

An efficient operator that extracts gradient information from an image is the multi-scale morphological gradient (MSMG), which shows the contrast level in the surrounding regions of a pixel. The MSMG technique is therefore utilised for picture segmentation and edge detection and is highly effective. As a focus measure, Multi-focus picture fusion has made use of MSMG. The information below is utilised for MSMG. A structural element with several scales is defined as

$$SE_j = SE_1 \oplus SE_2 \oplus \ldots . \oplus SE_N, j \in \{1,2, \ldots \ldots, N\} \quad (6)$$

The symbol for a basic structural element is SE1. The gradient feature Gt can be described using the morphological gradient operators shown in picture f.

$$G_t(x, y) = f(x, y) \oplus SE_t - f(x, y).SE_t \quad (7)$$

In contrast, (.) stands for the morphological operators for dilation and erosion, respectively. Here, t is the number of scales. The multi-scale structuring element can be extracted from the gradient feature by calculating the weighted sum of gradients on all scales. They are the same preprocessed images shown in Figure 2.

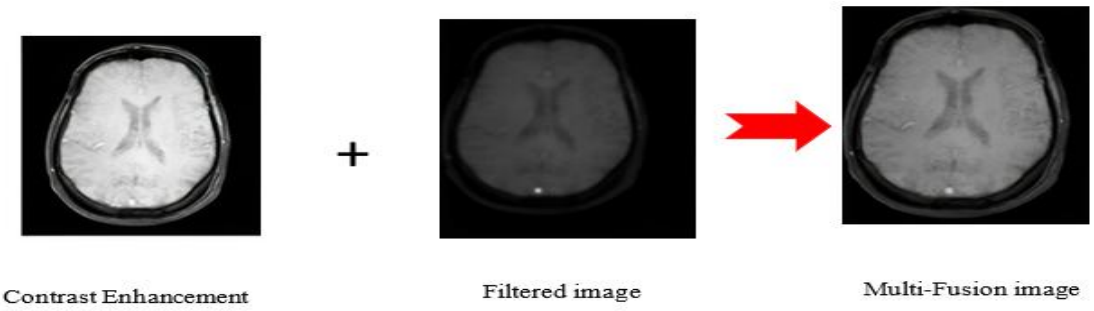

Figure 2: Sample image

$$M(x, y) = \sum_{t=1}^{N} w_t . G_t(x, y) \quad (8)$$

In this case, the gradient's weight on the t-th scale is indicated by

$$w_t = \frac{1}{2t+1} \quad (9)$$

3. Improved dwarf mongoose optimization algorithm (IDMO)

The IDMO algorithm's operation is explained in detail in this phase.

The IDMO mode

This optimisation method suggests the Improved Dwarf Mongoose Optimisation algorithm (IDMO) to improve DMO exploration and exploitation by altering the DMO in three straightforward but efficient ways: the IDMO chooses the alphas rather than the DMO, which chooses them solely on the basis of their computational load; the IDMO's alpha chooses the mongoose based on physical fitness; and a new operator is added to regulate the alpha's mobility. In order to expand the search and investigate previously unexplored locations, the scout group's movements are altered through randomisation. The three phases of the suggested method—ample food supply, forage space, and babysitters—achieve optimisation. The search agents are the individual mongooses as an n-by-d matrix.

During the exploration phase, the modified alpha guides the group to unexplored territory by adhering to the simulated processes. Randomisation is used to change the movements of scout groups in order to expand the search area and explore new areas. The exploitation is completed after the condition for babysitter swap is met and babysitters are switched. At this point, the acquired solution is improved to produce better outcomes.

Population initialization

Eq. (14) states that the IDMO population is stochastically initialised using a matrix of possible dwarf mongooses (X). The population vector is located between the upper bound (U) and lower bound (L) of the optimisation problem.

$$X = \begin{Bmatrix} x_{1,1} & x_{1,2} & x_1, d \\ . & : & : \\ x_{n,1} & x_{n,2} & x_{n,d} \end{Bmatrix} \quad (14)$$

Eq. (15) shows the location of the jth population's dimension for each Xi,jXi,j, where n is the total number of dwarf mongooses in a mound.

$$X_{i,j} = rand \times (U - L) + L \quad (15)$$

Alpha group

By subtracting the number of babysitters from the total number of dwarf mongooses, the overall population dimensions for this group are calculated. The alpha symbol in equation (16) indicates that the dwarf mongoose with the best match is chosen as the alpha.

$$\propto = \min(fit_1, fit_2 \dots \dots, fit_n) \quad (16)$$

Accuracy: The proportion of correct forecasts among all predictions is known as accuracy.

$$\text{Accuracy} = \frac{TP+TN}{TP+FP+TN+FN} \quad (17)$$

Sensitivity: Sensitivity, also referred to as recall or true positive rate (TPR), assesses a system's propensity to predict the future favourably.

$$TPR = \frac{TN}{TN+FP} \quad (18)$$

Specificity: Specificity, also known as true negative rate (TNR), assesses how well a system can predict unfavourable events.

$$TNR = \frac{TN}{TN+FP} \quad (19)$$

Precision: Precision, also known as positive prediction value (PPV), evaluates a system's ability to produce only pertinent results.

$$Precision = \frac{TP}{TP+FP} \quad (20)$$

F-Measure: The F-measure was used to calculate the harmonic mean of precision and recall.

$$\text{F} - \text{measure} = 2 * \frac{Re\ call * Precision}{Re\ call + precision} \quad (21)$$

The accuracy of the proposed model ranged from 0.98 to 0.99 in both testing and training. Table 1 displays the hyperparameter configuration.

Table 1: Optimized hyperpara meter used for training

Hyperparameter	Optimized value
Optimizer	Adam
No. of epochs	200
Batch size	32
Momentum	0.9
Decay	0
Learning rate	0.001

In Figures 6 and 7, the graphs show the IDS's loss value and categorisation accuracy as a function of iterations. The figure illustrates the good convergence effect of the study's methodology. For the purpose of training and testing the model, we split the dataset in half. The proposed strategy was trained in this phase using 200 training epochs of the processed training set. The learning rate that was set was 0.01.

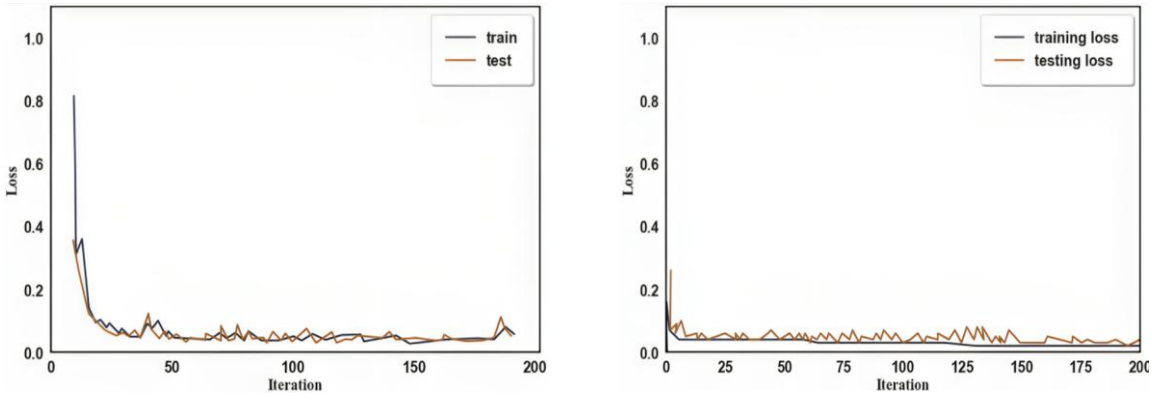

(A) (B)

Figure 3: Training vs Testing accuracy (A) training vs testing accuracy of PPMI dataset (B) training vs testing accuracy of NTUA dataset..

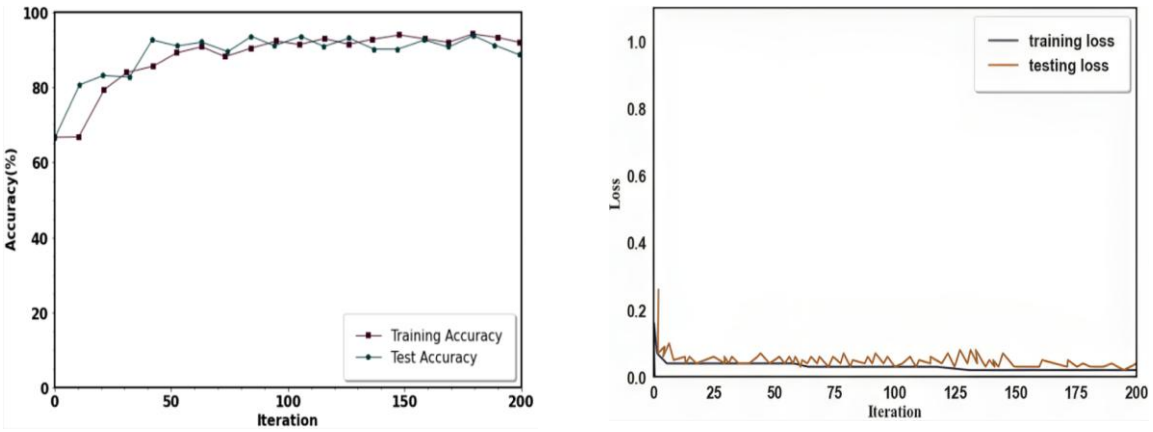

(A) (B)

Figure 4: Training vs Testing loss (A) training vs testing loss of PPMI dataset (B) training vs testing loss of NTUA dataset.

To penalise big weights in the network, it used L1 or L2 regularisation algorithms. By doing this, the model is less likely to fit the training data's noise. In order to lessen overfitting, Another regularisation technique called dropout randomly eliminates a subset of neurones while training. Your MobileNet model's width and depth may need to be decreased. It can investigate unique structures suited to the particular task or even employ smaller variations like MobileNetV3.

Table 8 shows a comparison of the current related works. While the previous writers used a variety of datasets, such as PD, PPMI, PD audio dataset, etc., our suggested method made use of PPMI and NTUA datasets. The suggested method performs better in terms of prediction when compared to current methods.

Table 2: Comparison of existing research with proposed.

References	Method	Dataset used	Accuracy	Sensitivity	Specificity
El Maachi, Bilodeau & Bouachir (2020)	1D-Convnet	PD dataset	94.1%	93.7%	96.8%
Loh et al. (2021)	2D-CNN	PD dataset	99.06%	98.22%	-
Ortiz et al. (2019)	Lenet 5 and AlexNet	PPMI	95.1%	-	-
Karaman et al. (2021)	Deep CNN	mPower voice database	89.75%	91.50%	88.40%
Diaz et al. (2021)	1D CNN and BiGRU	PaHaW and NewHandPD dataset	94.44%	98%	90%
Olivares et al. (2020)	ELM and BAT algorithm	Parkinson's disease audio dataset	96.7%	-	-
Vyas et al. (2022)	2D and 3D CNN	PPMI	88.9%	92%	92%
Proposed	Optimized MobileNetV3	PPMI and NTUA	99.3%	98.53%	99.12%

Conclusion

One of the most challenging medical diagnoses is Parkinson's disease. Although it is technically challenging to confirm a Parkinson's diagnosis, specialists can recognise the condition by assessing individuals and seeing a range of symptoms. Using the optimised MobileNet V3, the proposed study identified classes of Parkinson's illness based on MRI data. The Improved Dwarf Mongoose Optimisation algorithm (IDMO) was used to optimise the MobileNet V3 method. With accuracy of 99.34%, specificity of 99.12%, F-score of 97.78%, and sensitivity of 98.53%, respectively, the proposed

method outperformed the current methods. In earlier research, they used more calculation time to attain poorer precision. In order to achieve better classification accuracy than previous studies with less computational effort, the proposed methodology in this work combined deep learning-based feature extraction and optimised classification techniques. To find PD and other applications, it may be possible to look into hybridising techniques or developing new feature selection algorithms inspired by nature. Additionally, increasing the range of deep learning comparison methods will be essential.

References

Ghaeb, Jasim A., Malek Alkayyali, and Tarek A. Tutunji. "Wide range reactive power compensation for voltage unbalance mitigation in electrical power systems." Electric Power Components and Systems 49, no. 6-7 (2022): 715-728.

Brandao, Danilo I., Willian M. Ferreira, Augusto MS Alonso, Elisabetta Tedeschi, and Fernando P. Marafão. "Optimal multiobjective control of low-voltage AC microgrids: Power flow regulation and compensation of reactive power and unbalance." *IEEE Transactions on Smart Grid* 11, no. 2 (2019): 1239-1252.

Ganguly, Sanjib. "Multi-objective planning for reactive power compensation of radial distribution networks with unified power quality conditioner allocation using particle swarm optimization." *IEEE Transactions on Power Systems* 29, no. 4 (2014): 1801-1810.

Candra, Oriza, Mohammed I. Alghamdi, Ali Thaeer Hammid, José Ricardo Nuñez Alvarez, Olga V. Staroverova, Ahmed Hussien Alawadi, Haydar Abdulameer Marhoon, and M. Mehdi Shafieezadeh. "Optimal distribution grid allocation of reactive power with a focus on the particle swarm optimization technique and voltage stability." *Scientific Reports* 14, no. 1 (2024): 10889.

Boghdady, Tarek A., and Youssef A. Mohamed. "Reactive power compensation using STATCOM in a PV grid connected system with a modified MPPT method." *Ain Shams Engineering Journal* 14, no. 8 (2023): 102060.

Sarkar, Mohammad Nazmul Islam, Lasantha Gunaruwan Meegahapola, and Manoj Datta. "Reactive power management in renewable rich power grids: A review of grid-codes, renewable generators, support devices, control strategies and optimization algorithms." *Ieee Access* 6 (2018): 41458-41489.

Téllez, A. Águila, G. López, I. Isaac, and J. W. González. "Optimal reactive power compensation in electrical distribution systems with distributed resources. Review." *Heliyon* 4, no. 8 (2018).

Brandao, Danilo I., Willian M. Ferreira, Augusto MS Alonso, Elisabetta Tedeschi, and Fernando P. Marafão. "Optimal multiobjective control of low-voltage AC microgrids: Power flow regulation and compensation of reactive power and unbalance." *IEEE Transactions on Smart Grid* 11, no. 2 (2019): 1239-1252.

Salazar, Jair, Diego Carrión, and Manuel Jaramillo. "Reactive compensation planning in unbalanced electrical power systems." *Energies* 15, no. 21 (2022): 8048.

Kryonidis, Georgios C., Kyriaki-Nefeli D. Malamaki, Spyros I. Gkavanoudis, Konstantinos O. Oureilidis, Eleftherios O. Kontis, Juan Manuel Mauricio, José María Maza-Ortega, and Charis S. Demoulias. "Distributed reactive power control scheme for the voltage regulation of unbalanced LV grids." *IEEE Transactions on Sustainable Energy* 12, no. 2 (2020): 1301-1310.

Tadjeddine, Ali A., I. Arbaoui, H. Hamiani, and A. Chaker. "Optimal distribution of power under stress on power grid in real-time by reactive compensation-management and development in balance." *International Journal of Power Electronics and Drive Systems* 11, no. 2 (2020): 685.

Sarkar, Mohammad Nazmul Islam, Lasantha Gunaruwan Meegahapola, and Manoj Datta. "Reactive power management in renewable rich power grids: A review of grid-codes, renewable generators, support devices, control strategies and optimization algorithms." *Ieee Access* 6 (2018): 41458-41489.

ElMaachi, I., Bilodeau, G. A., & Bouachir, W. (2020). Deep 1D-ConvNet for accurate Parkinson's disease detection and severity prediction from gait. *Expert Systems with Applications, 143*(1), 113075.

Loh, H. W., Ooi, C. P., Palmer, E., Barua, P. D., Dogan, S., Tuncer, T., Baygin, M., & Acharya, U. R. (2021). GaborPDNet: Gabor transformation and deep neural network for Parkinson's disease detection using EEG signals. *Electronics, 10*(14), 1740.

Ortiz, A., Munilla, J., Martínez-Ibañez, M., Górriz, J. M., Ramírez, J., & Salas-Gonzalez, D. (2019). Parkinson's disease detection using isosurfaces-

based features and convolutional neural networks. *Frontiers in Neuroinformatics, 13*, 48.

Karaman, O., Çakın, H., Alhudhaif, A., & Polat, K. (2021). Robust automated Parkinson's disease detection based on voice signals with transfer learning. *Expert Systems with Applications, 178*(1), 115013.

Diaz, M., Moetesum, M., Siddiqi, I., & Vessio, G. (2021). Sequence-based dynamic handwriting analysis for Parkinson's disease detection with one-dimensional convolutions and BiGRUs. *Expert Systems with Applications, 168*(12), 114405.

Olivares, R., Munoz, R., Soto, R., Crawford, B., Cárdenas, D., Ponce, A., & Taramasco, C. (2020). An optimized brain-based algorithm for classifying Parkinson's disease. *Applied Sciences, 10*(5), 1827.

Vyas, T., Yadav, R., Solanki, C., Darji, R., Desai, S., & Tanwar, S. (2022). Deep learning-based scheme to diagnose Parkinson's disease. *Expert Systems, 39*(3), e12739.